Materials Science & Engineering A 689 (2017) 298–305

Contents lists available at ScienceDirect

Materials Science & Engineering A

journal homepage: www.elsevier.com/locate/msea

Evaluation of high-temperature creep behavior in Inconel-713C nickel-based superalloy considering effects of stress levels

Mohammad Azadi[a,*], Mahboobeh Azadi[b]

[a] Faculty of Mechanical Engineering, Semnan University, Semnan, Iran
[b] Faculty of Materials and Metallurgical Engineering, Semnan University, Semnan, Iran

ARTICLE INFO

Keywords:
High-temperature creep lifetime
Inconel-713C nickel-based superalloy
Stress level effects
Fracture surface
Carbides morphology

ABSTRACT

In this article, high-temperature creep behavior of the Inconel-713C nickel-based superalloy, which has been utilized in turbine blades, has been investigated. Creep testing was carried out on standard specimens at 850 °C and under different stress levels. Experimental data demonstrated that the applied stress caused a reduction in the creep lifetime, as a power law. Besides, scanning electron microcopy images showed that the mentioned material had a brittle fracture with cleavage marks on the fracture surface of samples. In addition, optical microscopy images indicated the high effect of the applied stress on the carbides morphology. During higher the creep lifetime, the length of carbides increased parallel to the force direction and caused to produce the trans-granular fracture. Then also, the amount of the γ' phase enhanced in the γ matrix, which caused to strengthen the creep resistance of the material.

1. Introduction

Nowadays, superalloys have been widely used in manufacturing of turbine blades, which operate in hot sections, weather in turbo-chargers of combustion engines or in gas turbines of aero engines. The application in aviation and automotive industries is due to excellent properties of superalloys, especially at high temperatures. In other words, superalloys could work at high temperatures, close to their solvus temperature, where they have to withstand mechanical loads [1,2].

According to the rotational speed of blades, the centrifugal force is induced in the material, where operating at high temperatures. Such loading leads to the creep phenomenon, which requires a constant load and high temperatures. Turbine blades are subjected to elevated temperatures under medium stresses for a prolonged time; therefore, the creep phenomenon will be a major mode of damages. Such creep deformation at high temperatures can lead to micro-cracking and the ultimate fracture; and therefore, is one of main mechanisms that limits the component lifetime, besides thermo-mechanical fatigue damages [1,2]. For designing such costly high-reliable parts, knowing the creep behavior has an important rule. Therefore, several researches have been represented on the creep behavior of superalloys, besides investigating related failure mechanisms.

Abu-Haiba et al. [3] studied the creep deformation and the monotonic stress-strain behavior of Haynes-556 superalloy at elevated temperatures, using analytical models. However, results of the θ projection method were accurate predictions of the rupture lifetime; while the Garofalo model over-estimated them. Hou et al. [4] presented the microstructure and mechanical properties of the cast Ni-based K44 superalloy. They demonstrated that tensile properties and creep behaviors had abnormal variations with increasing the temperatures, and the creep data could be fitted well with the modified Dyson-McLean relation. Marahleh et al. [5] predicted the creep lifetime of service-exposed turbine blades by the Larson-Miller parameter. They indicated that the rupture lifetime of specimens decreased with increasing the blade service lifetime. Also, the creep strain increased with increasing the service lifetime of blades at all test conditions. Kuo et al. [6] studied ageing effects on the microstructure and the creep behavior of the Inconel-718 superalloy. They showed that the γ phase was precipitated under control at the ageing temperature of 955 °C and various ageing times.

Chomette et al. [7] reported the effect of the initial microstructure on the Inconel-617 superalloy creep behavior at 850 °C and 950 °C. The preliminary cold work treatment highly reduced the strain rate of the material and also enhanced the creep lifetime at 850 °C, while the opposite was observed at 950 °C. Liu et al. [8] investigated the creep damage mechanism and the γ' phase morphology of a V-notched round bar in Ni-based single crystal superalloys. They indicated that damages initiated at the inner material and propagated to the free surface in the smooth specimen, while cracks initiated at the notch root and the final

* Corresponding author
E-mail address: m_azadi@semnan.ac.ir (M. Azadi).

http://dx.doi.org/10.1016/j.msea.2017.02.066
Received 28 September 2016; Received in revised form 14 December 2016; Accepted 17 February 2017
Available online 20 February 2017
0921-5093/

fracture occurred at the center region in the notched specimen. Tian et al. [9] represented damage and fracture mechanisms of a nickel-based single crystal superalloy during creep testing at moderate temperatures. Their results indicated that the deformation mechanism was dislocations slipping in the γ matrix and shearing into the γ' phase. Lu et al. [10] investigated the creep rupture of the GH4169 superalloy under a constant load and at 550 °C and 700 °C. They demonstrated that stress rupture damages in the material started from the incoherent interface between the δ phase and grain boundaries; and then finally linked together to produce the inter-granular fracture.

Wollgramm et al. [11] presented the creep behavior of a Ni-based single crystal superalloy to show the dependency of the stress and the temperature to the minimum creep rate, as a power law type and as an exponential type, respectively. The stress exponent increased with increasing the stress and decreasing the temperature, while higher apparent activation energies were observed for lower stresses and higher temperatures. Lee et al. [12] represented a new approach to strengthen grain boundaries for the creep improvement of a Ni-Cr-Co-Mo superalloy at 950 °C. That research verified that as compared to the standard condition, the creep resistance could be extended to be 2.8 times longer by the combination of the grain boundaries serration and the preliminary cold deformation.

According to the literature review, researches on the Inconel-713C nickel-based superalloy have been performed rarely and still needs to impress on the creep behavior of the alloy. Therefore, in this article, 713C superalloys specimens were tested under creep loading at 850 °C and in different stress levels. Then, the creep behavior of the material was studied through curves of the strain and the strain rate. In addition, failure mechanisms were evaluated by the scanning electron microscopy (SEM) method.

2. Materials and experiments

In this research, the case study is the Inconel-713C nickel-based superalloy. The application of this material is in turbine blades manufacturing, in the turbo-charger component of a national engine in Iran. The chemical composition of the studied material is depicted in Table 1, compared to the standard [13]. Measured values, mentioned in Table 1, represented a good agreement with values in the standard.

In this article, creep tests were performed under high temperatures and through a constant load, according to the standard: ASTM-E139-11 [14]. The specimen geometry and utilized equipments can be found in Figs. 1 and 2, respectively. Specimens were prepared from a casted Inconel-713C nickel-based superalloy cylinder. Standard samples were machined from some thinner cylinders, which were produced by wire cutting from the casted material.

As it can be seen in Fig. 2, creep test equipments (SANTAM Company, SCT-300 creep testing machine) include the frame, grips, weights for loading, the extensimeter, thermo-couples, the furnace, the temperatures panel, the load cell and the load-arm, which ratio is 1–10. The load and displacement were measured by the load cell and the extensometer, respectively. Besides, the temperature was measured by K-type thermo-couples. Then, the stress was calculated from the load,

Table 1
The chemical composition of the studied material.

Element	Measured values	Composition in Ref. [3]	Element	Measured Values	Composition in Ref. [3]
Ni	balance	balance	C	0.12	0.08–0.20
Al	5.50	0.05–0.50	Fe	0.13	max 2.50
Ti	0.97	0.50–1.00	B	0.01	0.01–0.02
Ta+Nb	1.91	1.80–2.80	Zr	0.06	0.05–0.15
Mn	0.04	Max 0.25	Si	0.04	max 0.50
Cr	14.00	12.00–14.00	Cu	0.01	max 0.50
Mo	4.50	3.80–5.20	V	trace	trace

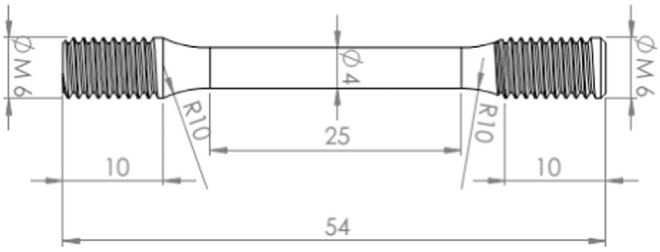

Fig. 1. : The specimen geometry (in millimeter) under creep testing.

the area of the specimen cross-section and the ratio of the load arm. In addition, the strain was calculated from the displacement and the initial length of the specimen. In this case, two types of the strain including the true strain ($\varepsilon_t=ln(l/l_0)$) and the engineering strain ($\varepsilon_e=\Delta l/l_0$) could be reported, where l is the length during testing, l_0 is the initial length and Δl is the difference between the length and the initial length ($\Delta l = l-l_0$). In this research, since two curves had a similar behavior, only true values were depicted.

Since the temperature of fluids and solids in the turbo-charger component in a specified combustion engine is around 950 °C and 850 °C, respectively [15]; the temperature test was considered as 850 °C in all creep testing. It should be mentioned that the activation temperature for the creep in metals is 35–50% [16] or 30–40% [17] of the melting point. Then also, low and high temperature creep phenomena are considered as 40% and 50% of the melting point, respectively [18]. As the solvus temperature of the Inconel-713C nickel-based superalloy is about 1260 °C [19]; therefore, 850 °C creep testing is here a high temperature creep phenomenon in the material.

For stress levels, applied loads included 65, 70 and 75 kg, equaled to 507.7, 546.7 and 585.8 MPa. It should be noted that under larger stress value, the creep test was repeated for investigating the repeat-

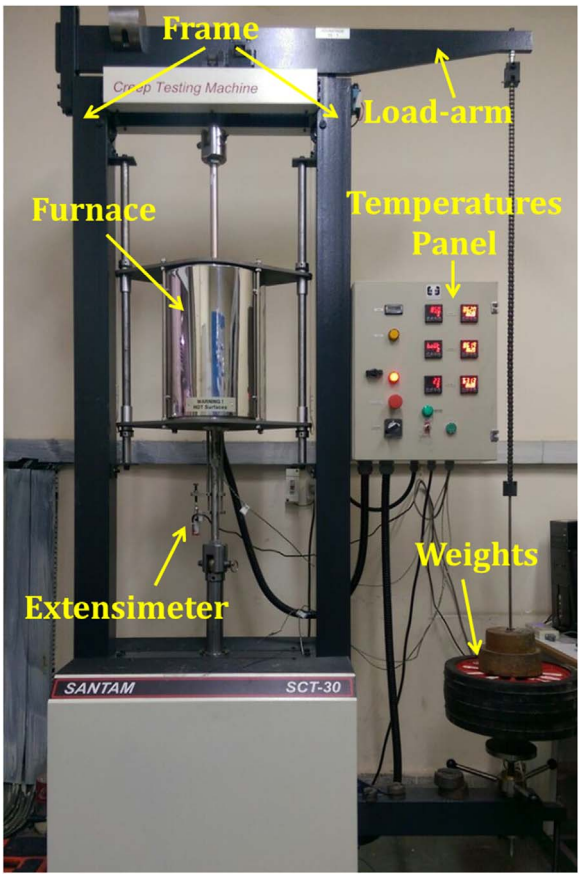

Fig. 2. : Creep tests equipments including grips, the furnace and the load arm.

ability of testing. Such stress levels were selected based on the maximum rotational speed of the turbine, which is 220000 rpm in a specified combustion engine [15]. Therefore, investigating the stress level influence on the creep behavior of the material would be comparable to study the effect of the turbine speed.

To study the fracture surface, the SEM equipment (the XLC-Philips model) was utilized with the accelerated voltage of 20 kV. Besides, the energy dispersive X-ray spectroscopy (EDS) was used to show the local chemical composition of different phases. In addition, an optical microscopy (the Olympus model) was also used for observing the micro-structure (including the carbides distribution) of samples, before and after creep testing.

3. Results and discussions

3.1. Micro-structures before testing

Fig. 3 shows typical images of the Inconel-713C nickel-based superalloy microstructure, in the as-cast state in two magnifications (200X and 500X). Fig. 3(a) demonstrates the distribution of alloy carbides in the γ phase matrix. Different carbides with an irregular shape had the maximum length and the thickness of about 150 and 20 μm, respectively. Fig. 3(b) presents the rounded morphology of the γ' phase, in the γ phase matrix. In some regions, the γ' phase (black-colored regions in Fig. 3(b)) surrounded carbides (white-colored regions in Fig. 3(b)). Such behavior was also reported by the literature [20]. In addition, in the γ matrix, the γ' phase was distributed as an inter-metallic phase between nickel and titanium. The size of the γ' phase was approximately less than 10 μm, which is responsible for the contributions of coherency strain hardening [21,22]. Small γ' phase precipitates always occur as a sphere or rounded phase. When the γ' phase increases to 70% of the matrix, the phase shape would change to the cubic form. The enhancement of directional coarsening causes lattice mismatches [23]. In some regions of the microstructure, this phase had surrounded carbides.

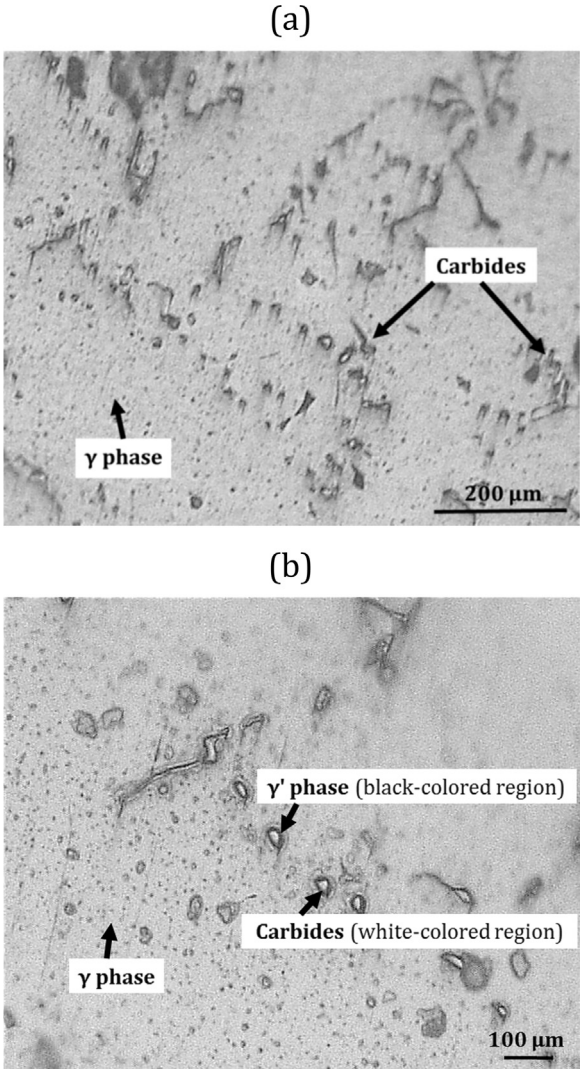

Fig. 3. : The microstructure of the as-cast Inconel-713C nickel-based superalloy, before the creep test by the optical microscope, with magnifications of (a) 200X and (b) 500X.

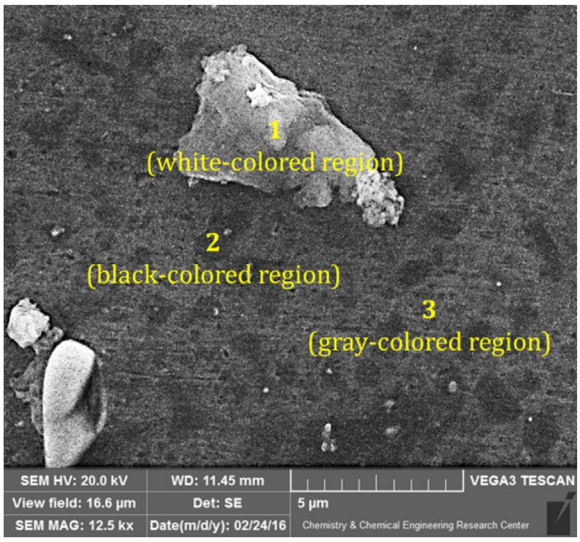

Fig. 4. : The SEM image of the as-cast Inconel-713C nickel-based superalloy, before the creep test.

The SEM image of the as-cast Inconel-713C nickel-based superalloy, before creep testing, can be seen in Fig. 4. Besides, Table 2 includes EDS results for different regions (phases), shown in Fig. 4. According to Table 2 for EDS results, Region No. 1 in Fig. 4 (includes the white-colored area) depicted carbides. The carbides type contains chrome, titanium and niobium elements, which are stabilized at high temperatures [6,13]. Region No. 2 in Fig. 4 (includes the black-colored area) shows the γ'-$Ni_3(Al,Ti)$ phase. The averaged diameter of the γ' phase was about 1 μm. Region No. 3 in Fig. 4 (includes the gray-colored area) demonstrates the γ phase. It should be noted that the γ phase is a nickel solid solution with other elements such as chrome and molybdenum. It should be noted that the γ' phase and carbides are generally significant for strengthening the material and improve mechanical properties. Besides, they make grain boundaries stable and increase the strength at high temperatures [20].

Table 2
EDS results for the local chemical composition of phases, shown in Fig. 4.

Element	Region No. 1		Region No. 2		Region No. 3	
	Atomic percent	Weight percent	Atomic percent	Weight percent	Atomic percent	Weight percent
Al	1.75	1.35	16.79	9.31	0.75	0.35
Ti	6.46	6.20	7.99	7.20	0.16	0.13
Cr	8.27	8.99	3.49	2.83	5.27	4.70
Ni	48.30	51.97	71.02	80.66	93.30	93.97
Mo	–	–	–	–	0.52	0.85
C	12.99	8.56	–	–	–	–
Nb	22.23	22.96	–	–	–	–

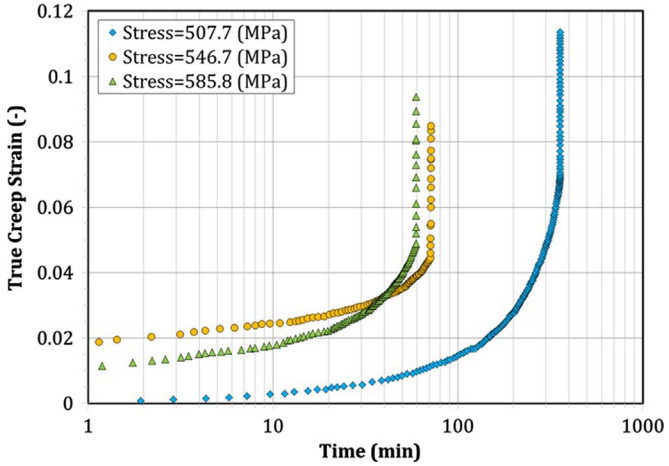

Fig. 5. : Curves of the true creep strain versus the time for the Inconel-713C nickel-based superalloy.

3.2. Strains and strain rates during testing

Curves of the creep strain and the creep strain rate, both versus the time, are presented in Figs. 5 and 6, respectively. It should be mentioned that the time is in a logarithmic scale to show obtained results in a proper state. As another note, although the repeated creep test was performed at 850 °C and under 585.8 MPa for checking the repeatability of testing; but only one of repeated creep tests was shown in these figures. For more details, the creep lifetime and the minimum strain rate are reported in Table 3, based on true strain values. Here, obtained results of both repeated creep tests (at 850 °C and under 585.8 MPa) are depicted.

As it can be seen in Fig. 5, the true creep strain started about zero under low stresses, as 507.7 MPa. Under higher stresses, the initial value of the strain was about 0.01–0.02. As known, three stages can be defined in the relation between the creep strain and the time. For all curves in Fig. 5, it was difficult to observe the primary stage of the creep behavior. However, the second stage and the third stage could be seen under different stress levels. Such behavior (no observing the primary stage of the creep behavior) was also reported by other researches [12,24,25] for different superalloys. From Fig. 6, it can be found that higher strain rate occurred at the initial time of the creep lifetime. When the applied stress increased, the strain rate increased also in first times.

Based on obtained results in Table 3, the creep lifetime of the Inconel-713C nickel-based superalloy decreased by increasing the applied stress, as expected. In other words, increasing 7–8% in the amount of applied stresses caused to 17–80% reduction of the creep lifetime. Such lifetime decrease was more significant under lower applied stresses. Besides, the minimum creep strain rate of the material increased, when the applied stress enhanced. This behavior showed a direct relation between the stress and the strain rate. Increasing 7–8% of the stress was equal to 27–364% enhancement in the minimum creep strain rate. This property improvement was higher when the applied stress was in lower levels. Such trends demonstrated a power law between the strain rate and the lifetime and also between the stress and the lifetime, in the Inconel-713C nickel-based superalloy. Mentioned relations can be found in Fig. 7, with the reported coefficient of determination for best curve fitting. Based on these results, the coefficient of determination was 87% and 99% for the applied stress-creep lifetime curve and the creep strain rate-creep lifetime curve, respectively. In addition, following relations could be represented for the Inconel-713C nickel-based superalloy,

$$\sigma = 767.9(N_c)^{-0.071} \quad (1)$$

$$\dot{\varepsilon}_{min} = 0.0539(N_c)^{-1.021} \quad (2)$$

where, N_c is the creep lifetime, σ is the applied stress, and $\dot{\varepsilon}_{min}$ is the minimum creep strain rate. Mentioned formulations indicated a reverse relation between the stress and the creep lifetime and also between the minimum strain rate and the creep lifetime.

Table 3
Creep results of the Inconel-713C nickel-based superalloy.

Temperature (°C)	Applied stress (MPa)	Creep lifetime (min)	Minimum creep strain rate (1/min)
850	507.7	358.5	0.000135
850	546.7	71.4	0.000627
850[a]	585.8[a]	59.6	0.000798
850[a]	585.8[a]	53.3	0.001045

[a] The repeated creep test at 850 °C and under 585.8 MPa for checking the repeatability of testing. More details can be found at the end of the part "Results and Discussions".

3.3. Micro-structures after testing

Fig. 8 shows optical microscopy images of different samples, before and after the creep test. For all samples, shown in Fig. 8(a), (b) and (c), the irregular shape of carbides was seen in the cross section view, without any preferred orientation. Whereas Fig. 8(d), (e) and (f) shows

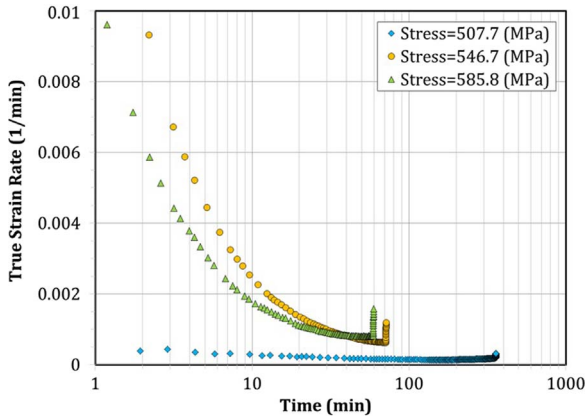

Fig. 6. : Curves of the true creep strain rate versus the time for the Inconel-713C nickel-based superalloy.

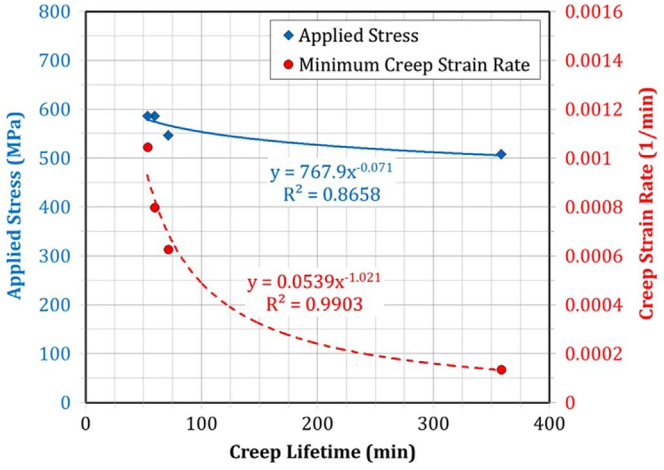

Fig. 7. : Curves of the applied stress versus the creep lifetime and the creep strain rate versus the creep lifetime for the Inconel-713C nickel-based superalloy.

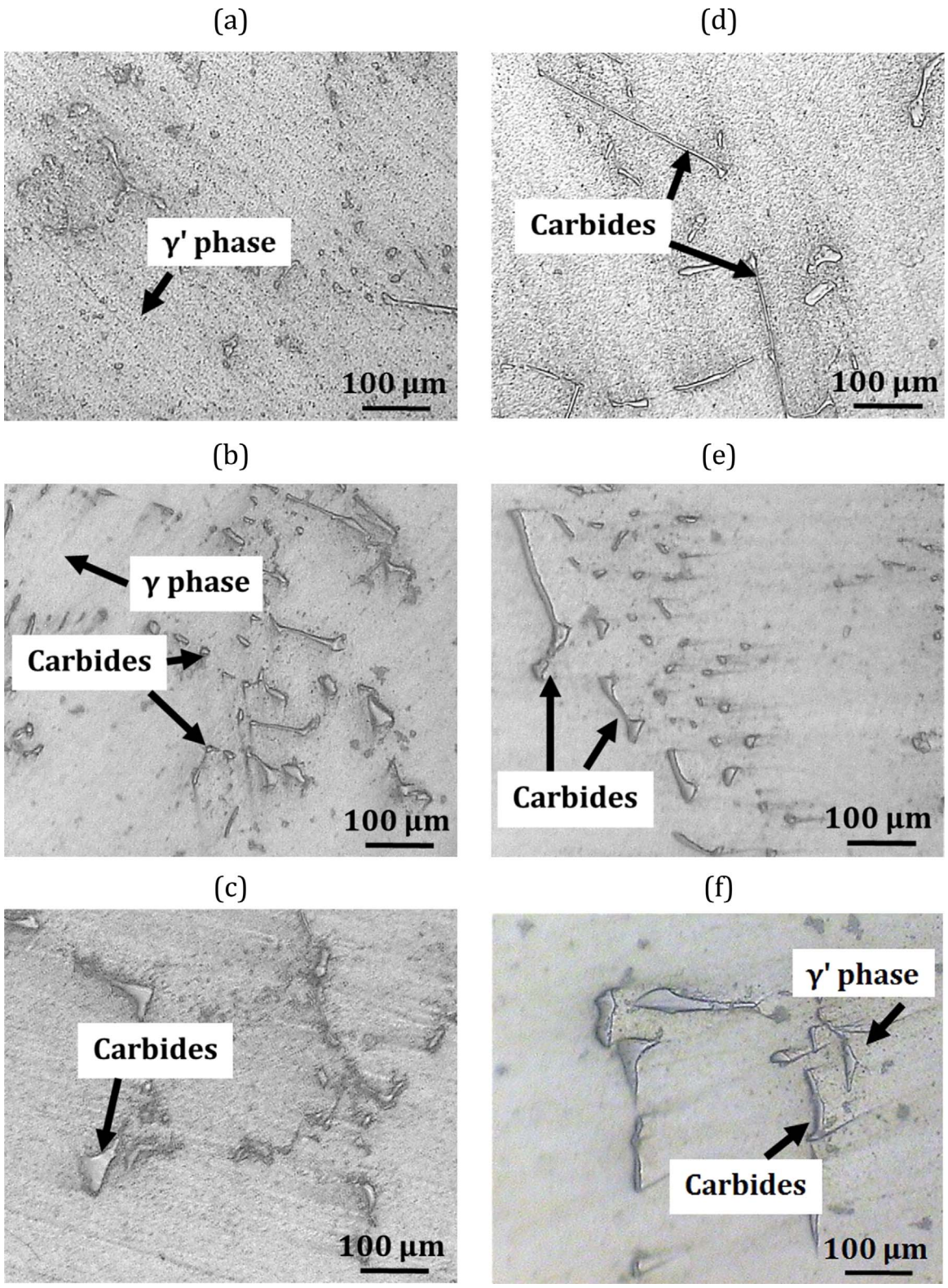

Fig. 8. : The microstructure of the Inconel-713C nickel-based superalloy after testing by the optical microscope including (a), (b) and (c) for the cross section of specimens, vertical to the force direction and (d), (e) and (f) in the length direction of specimens, parallel to the force direction; for creep tests under (a) and (b): 507.7 MPa, (c) and (d): 546.7 MPa, and (e) and (f): 585.8 MPa.

the directional morphology of carbides, in the Inconel-713C nickel-based superalloy, after creep tests. This result was in convenience with results, presented by Lu et al. [10]. The morphology of carbides changed to the one-dimensional shape (like the acerate). Besides, the maximum length of carbides increased even to about 300 µm and then, the carbides thickness decreased. The applied stress affected the carbides morphology, as the rupture time changed. As shown in Fig. 8(d), the maximum increased length of carbides was related to

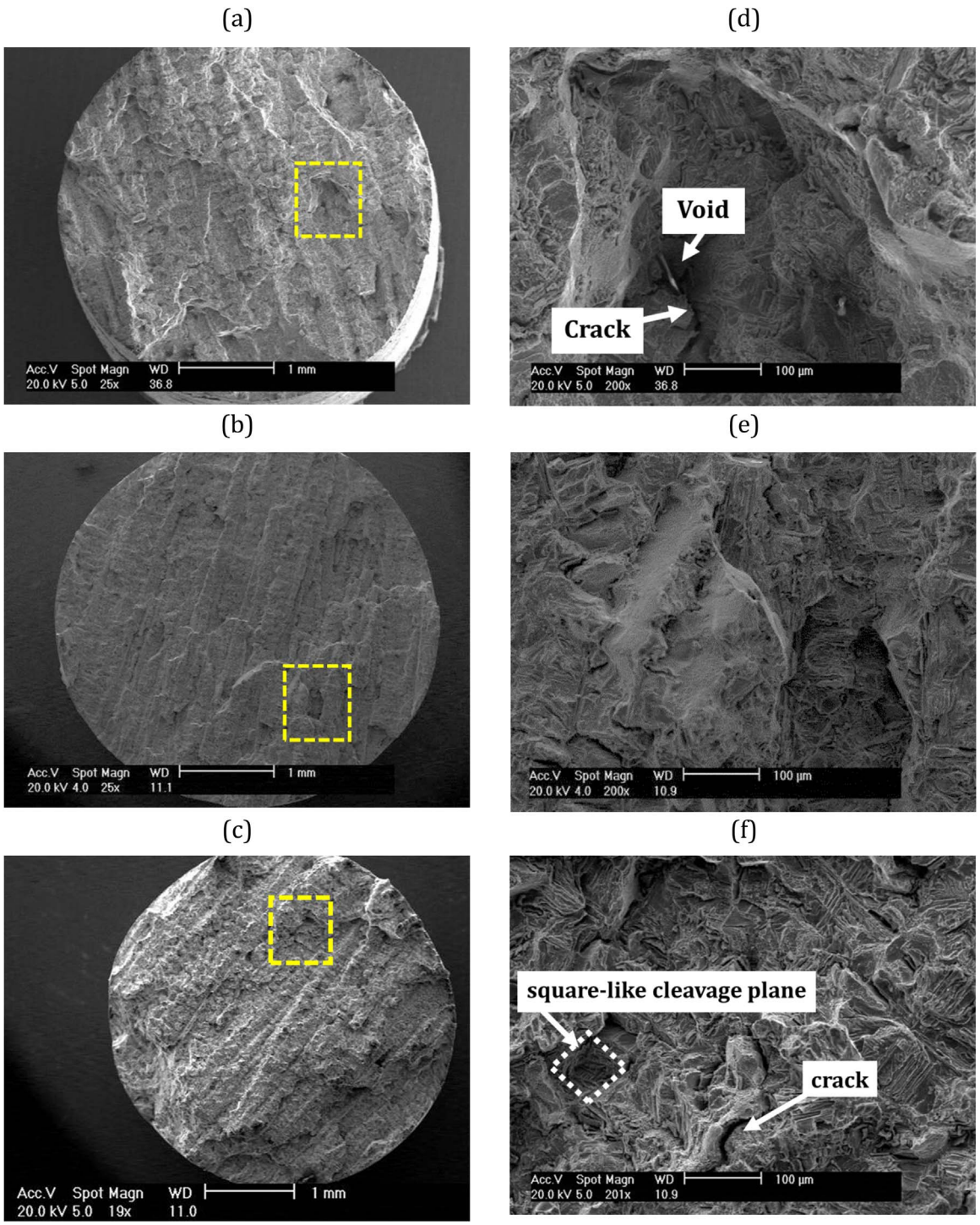

Fig. 9. : The fracture surface of the as-cast Inconel-713C nickel-based superalloy after testing by the SEM, for creep tests under (a) and (d): 507.7 MPa, (b) and (e): 546.7 MPa, and (c) and (f): 585.8 MPa (Note: The square in left images shows the place of right images.).

the creep test under 507.7 MPa (lower stress level), since the diffusion time was long.

The γ' phase was also seen obviously in the sample under 507.7 MPa, due to the more maintaining time at 850 °C. The γ' phase solvus temperature (more than 1260 °C) would provide high creep strength [26], as the crystal plane of the γ' phase was in the registry of the γ phase matrix. The close match (0–1%) between the lattice parameter of the matrix and precipitates, besides the chemical compatibility, allowed the γ' phase to precipitate homogenously and coherently, throughout the matrix. Therefore, the γ' phase had a long-time stability. In addition, the γ' phase was absolutely ductile and thus; enhanced the strength of the γ phase matrix, without lowering the fracture toughness [23]. On the other hand, the γ' phase acted as a barrier to the dislocation motion to lower the speed of the motion, within a crystal structure. As the stress increased to 585.8 MPa (higher stress level), the presence of the γ' phase was limited between carbide branches, due to the short time of the creep test, shown in Fig. 8(e) and (f).

Matysiak et al. [27] reported that the rafting behavior of the γ' phase, after creep testing for the Inconel-713C nickel-based superalloy. It should be noted that their temperature condition was 980 °C and the

creep rupture time was longer than 25 h, under 150 MPa. However, in this research, the temperature and the rupture time were lower than those values in the literature [27]. According to this condition, such rafting behavior of the γ' phase, after creep testing was not observed, especially for creep tests under 546.7 and 585.8 MPa, which specimens had lower creep lifetimes. For proving this claim accurately, more investigations should be performed by SEM images.

3.4. Fracture surfaces after testing

The SEM fractography of all specimens is shown in Fig. 9, under different stress levels. All fracture surfaces showed a brittle damage, as reported by Lu et al. [10]. Various big creep voids were observed in the cross section of samples, after the rupture, especially in the sample under 507.7 MPa (lower stress level). When the load increased to 585.8 MPa (higher stress level), the pattern of SEM images became different. The shape of fractured cross sections for all specimens was near a circular mode, and not like elliptic and the inclined shape. Such results can be seen in the literature [28]. Indeed, for specimens crept at 850 °C, a uniform and moderated reduction in the area on the whole gauge length was seen for all samples.

The shape of failures in the fracture surface was like bumps and indents (such as cleavage marks). This failure showed that the fracture occurred in different crystal planes, especially in the middle of the cross section in samples. Besides twinning and dislocation mechanisms, grain boundary sliding was also activated during creep testing. Some creep damages were started from the incoherent interface between carbides and the matrix. Finally, this event produced the trans-granular fracture. The grain boundary was attributed to the damage initiation [6].

Despite the observed brittle behavior in this article, in some other cases, researchers [24,25] reported the ductile behavior of superalloys, where high temperatures were considered for creep testing. Zhao et al. [24] showed that the fracture surface of Cr25Ni35Nb and Cr35Ni45Nb alloys revealed the ductile fracture behavior, which was characterized by the presence of dimples. The reason could be due to the temperature of creep testing, which was 950 °C and under 50 MPa. Liu et al. [25] illustrated that the fracture initiated from the center of the cross section of specimens, by appearing the character of small and shallow dimples. Again, the creep testing condition was at 980 °C and 400 MPa.

It may be understood from Fig. 9(c) that edge lines in the square-like cleavage plane was parallel to {110} directions. The {110} direction in the FCC crystal was the close packed direction and dislocations were easily activated along the direction, due to the higher elastic modulus than that of the {100} direction. Therefore, the elastic strain energy maybe released, when the crack was propagated along the direction. This phenomenon suggested that the {110} direction in the FCC crystal possessed the bigger probability of the crack propagation. The strain value of the alloy increased as the creep went on and significant amounts of dislocations were activated to bring the stress concentration. This may promote the propagation of the hole-like crack along the {110} direction, on the (001) plane, under the action of applied loading at high temperatures [9].

3.5. The repeatability of testing

The repeatability of creep testing is shown in Fig. 10, including the true creep strain and the true creep strain rate, both versus the time. Results in this figure were obtained under 585.8 MPa at 850 °C. As it can be seen in Fig. 10, the trend of results in Test 1 and Test 2 was similar. Under such loading condition, the creep lifetime was measured as 56.5 ± 3.6 h and the minimum true creep rate was measured as 0.000923 ± 0.000124 1/min. mentioned results demonstrated a good repeatability, where the ratio of the deviation amount to the averaged value was small, as 6% and 13% for the creep lifetime and the creep strain rate, respectively.

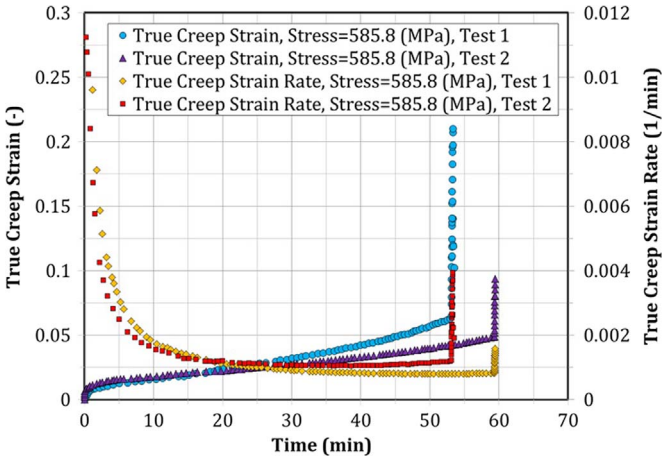

Fig. 10. : Curves of the true creep strain and the true creep strain rate, both versus the time for the Inconel-713C nickel-based superalloy.

4. Conclusions

This article has represented the creep behavior of a nickel-based superalloy used in turbine blades at 850 °C, under different stress levels. Such investigations in the literature review on the Inconel-713C nickel-based superalloy were rare in comparison to other superalloys. Then, experimental data demonstrated following results,

- The enhancement of the applied stress decreased the creep lifetime, with a power law. When the amount of the stress level increased as 7–8%, the reduction of the creep lifetime was 17–80% in the material. Besides, the true creep strain rate had also a power relation with the lifetime.
- The carbides morphology was significantly affected by the applied stress. Increasing the creep time caused an increased in the length of carbides, parallel to the force direction. Besides, the γ' phase was more precipitated in the matrix.
- Brittle damages could be observed on fracture surfaces of all specimens. In addition, cleavage marks were significant as a failure mechanism during creep testing in all samples.
- The repeatability of creep testing indicated a small deviation in results of the lifetime and the minimum strain rate. Therefore, the uncertainty of results in creep testing was small for the Inconel-713C nickel-based superalloy at 850 °C.

Acknowledgement

Authors would thank to Semnan University in Semnan, Iran, according to the financial support, based on a research project (No. 266/95/234).

References

[1] D. Hollander, D. Kulawinski, M. Thiele, C. Damm, S. Henkel, H. Biermann, U. Gampe, Investigation of isothermal and thermo-mechanical fatigue behavior of the nickel-base superalloy IN738LC using standardized and advanced test methods, Mater. Sci. Eng. A 670 (2016) 314–324.
[2] K.O. Lee, K.H. Bae, S.B. Lee, Comparison of prediction methods for low-cycle fatigue life of HIP superalloys at elevated temperatures for turbopump reliability, Mater. Sci. Eng. A 519 (2009) 112–120.
[3] M.S. Abu-Haiba, A. Fatemi, M. Zoroufi, Creep deformation and monotonic stress-strain behavior of Haynes alloy 556 at elevated temperatures, J. Mater. Sci. 37 (2002) 2899–2907.
[4] J.S. Hou, J.T. Guo, L.Z. Zhou, C. Yuan, H.Q. Ye, Microstructure and mechanical properties of cast Ni-base superalloy K44, Mater. Sci. Eng. A 374 (2004) 327–334.
[5] G. Marahleh, A.R.I. Kheder, H.F. Hamad, Creep life prediction of service-exposed turbine blades, Mater. Sci. Eng. A 433 (2006) 305–309.
[6] C.M. Kuo, Y.T. Yang, H.Y. Bor, C.N. Wei, C.C. Tai, Aging effects on the microstructure and creep behavior of Inconel 718 superalloy, Mater. Sci. Eng. A

510–511 (2009) 289–294.
[7] S. Chomette, J.M. Gentzbittel, B. Viguier, Creep behavior of as received, aged and cold worked Inconel 617 at 850 °C and 950 °C, J. Nucl. Mater. 399 (2010) 266–274.
[8] D. Liu, Z. Wen, Z. Yue, Creep damage mechanism and γ' phase morphology of a V-notched round bar in Ni-based single crystal superalloys, Mater. Sci. Eng. A 605 (2014) 215–221.
[9] S. Tian, X. Ding, Z. Guo, J. Xie, Y. Xue, D. Shu, Damage and fracture mechanism of a nickel-based single crystal superalloy during creep at moderate temperature, Mater. Sci. Eng., A 594 (2014) 7–16.
[10] X. Lu, J. Du, Q. Deng, J. Zhuang, Stress rupture properties of GH4169 superalloy, J. Mater. Res. Technol. 3 (2) (2014) 1–8.
[11] P. Wollgramm, H. Buck, K. Neuking, A.B. Parsa, S. Schuwalow, J. Rogal, R. Drautz, G. Eggeler, On the role of Re in the stress and temperature dependence of creep of Ni-base single crystal superalloys, Mater. Sci. Eng. A 628 (2015) 382–395.
[12] J.W. Lee, D.J. Kim, H.U. Hong, A new approach to strengthen grain boundaries for creep improvement of a Ni-Cr-Co-Mo superalloy at 950 °C, Mater. Sci. Eng. A 625 (2015) 164–168.
[13] M.J. Donchie, S.J. Donchie, Superalloys: a technical guide, ASM International, 2002.
[14] Standard test methods for conducting creep, creep-rupture and stress-rupture tests of metallic materials, ASTM International, 2012.
[15] Technical Reports on Turbo-charger, Irankhodro Powertrain Company, Tehran, Iran, ⟨www.ip-co.ir⟩.
[16] T. Gocmez, A. Awarke, S. Pischinger, A new low cycle fatigue criterion for isothermal and out-of-phase thermo-mechanical loading, Int. J. Fatigue 32 (2010) 769–779.
[17] R. Minichmayr, Modeling and simulation of thermo-mechanical fatigue behavior of aluminum components (Ph.D. thesis), University of Leoben, Leoben, Austria, 2005.
[18] W.F. Smith, Foundation of Materials Science and Engineering, McGraw-Hill, 2003.
[19] Engineering properties of alloy 713C, Technical Literature, No. 337, Nickel Institute, Belgium.
[20] S. Petronic, A. Milosavljevic, Heat treatment effect on multicomponent nickel alloys structure, Fac. Mech. Eng. Trans. 35 (2007) 189–193.
[21] M.G. Burke, M.K. Miller, Precipitation in alloy 718: A combined AEM and APFIM investigation, Special Emphasis Symposium on Superalloys 718, 625 and Various Derivatives, Pittsburgh, USA 23–26, 1991.
[22] M. Sundararaman, P. Mukhopadhyay, S. Banerjee, Precipitation and room temperature deformation behavior of Inconel 718, Special Emphasis Symposium on Superalloys 718, 625 and Various Derivatives, Pittsburgh, USA 419–440, 1991.
[23] R. Bowman, Superalloys: A primer and history, 9th International Symposium on Superalloys, Pennsylvania, USA 17–21, 2000.
[24] Y. Zhao, J. Gong, J. Yong, X. Wang, L. Shen, Q. Li, Creep behaviors of Cr25Ni35Nb and Cr35Ni45Nb alloys predicted by modified theta method, Mater. Sci. Eng. A 649 (2016) 1–8.
[25] D. Liu, Z. Wen, Z. Yue, Creep damage mechanism and γ' phase morphology of a V-notched round bar in Ni-based single crystal superalloys, Mater. Sci. Eng. A 605 (2014) 215–221.
[26] M. Gel, D.N. Duhl, A.F. Giamei, The development of single crystal superalloy turbine blades, Superalloys (1980) 205–214.
[27] H. Matysiak, M. Zagorska, A. Balkowiec, B. Adamczyk-Cieslak, R. Cygan, J. Cwajna, J. Nawrocki, K.J. Kurzydłowski, The microstructure degradation of the IN 713C nickel-based superalloy after the stress rupture tests, J. Mater. Eng. Perform. 23 (9) (2014) 3305–3313.
[28] S. Zhang, J. Zhang, L. Lou, Anisotropic creep rupture properties of a nickel-base single crystal superalloy at high temperature, J. Mater. Sci. Technol. 27 (2) (2011) 107–112.